THE ROLE OF ENDOPLASMIC RETICULUM STRESS IN THE IMMUNE RESPONSE TO CANCER

Natalia Lopez-Barbosa

ABSTRACT

Current studies of malignant tumors are performed in xenograft models that consist of cancerous tumors grown in immunosuppressed mice. Although this has been the standard for years, this model ignores the immunological content of the tumor microenvironment. For this reason, little is known about the reasons behind the failure to clear cancer by the immune system, which might be correlated with the limiting effect that CAR-T-based immunotherapies have shown in solid tumors. Here I present a mathematical model of the IRE1α-XBP1 arm of the UPR in T lymphocytes when exposed to ascites within the tumor microenvironment. The model correlates with experimental data measured by Song et al. [7]. Parameter sensitivity analysis suggests that inhibition of the transcription and translation of IRE1 could alleviate the immunosuppressing behavior of tumor-infiltrating T cells.

INTRODUCTION

When under cellular stress, the failure of different endogenous processes can lead to malfunction, damage or cellular death. One example of this is the cellular stress that arises from the accumulation of misfolded proteins in the endoplasmic reticulum (ER), which is commonly referred to as ER stress. After transcription and translation take place, polypeptides are transported to the ER through the SEC61 channel to undergo protein folding and post-translational modifications such as disulphide-bond forming and N-linked glycosylation. Any failure in these events can lead to ER stress, causing the cell to activate what is known as the unfolded-protein response (UPR) [1].

The UPR activates three different pathways that help the cell alleviate the accumulation of misfolded proteins. These pathways are governed by three distinct ER-transmembrane proteins: the inositol-requiring transmembrane kinase/endonuclease 1 (IRE1) [2], the pancreatic ER kinase (PERK) [3] and the activating transcription factor 6 (ATF6) [4]. In the absence of ER stress, the three proteins are encountered in an inactive state controlled by their association with an immunoglobin-heavy-chain binding protein (BIP).

In the tumor microenvironment, malignant cells favor glycolysis by rapidly using the available glucose and glutamine even in the presence of abundant oxygen species in what is known as the Warburg effect [5]. This limits the availability of these nutrients for neighboring immune cells, compromising the hexosamine biosynthetic pathway and conditioning N-linked protein glycosylation. This, coupled with a decrease in their surrounding pH due to the secretion of lactate by cancerous cells [6], triggers the UPR in tumor-infiltrating immune cells.

Among the different types of immune cells encountered within the tumor microenvironment, functional T lymphocytes provide immune pressure against cancer by releasing cytotoxins and providing long-term immune responses towards cancerous cells. Nonetheless, Song et al. [7] showed that ovarian-cancer-associated T cells are under ER stress as measured by an increase in the expression of spliced XBP1 (XBP1s), limiting their effectiveness. Here, I present a mathematical model of the IRE1α-XBP1 cascade presented in Figure 1. The model emulates the effect of ascites in the activation of the UPR in T cells as shown in [7]. After proving a similar behavior with respect to experimental data, I provide an analysis on which parameters affect the most the expression of XBP1s.

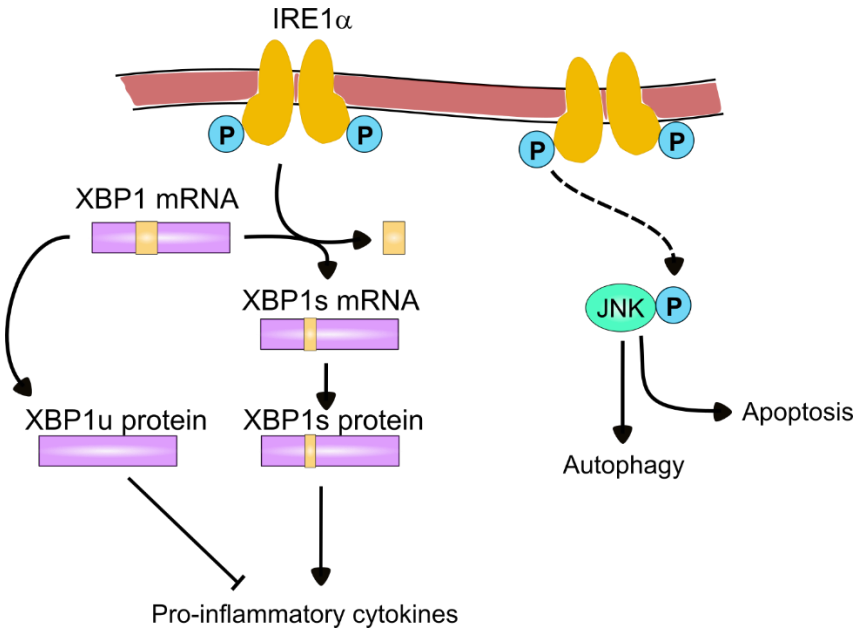

Figure 1. IRE1α-XBP1 signal cascade. Accumulation of unfolded proteins in the ER lumen promotes the release of BIP, allowing homodimerization and activation of IRE1. Phosphorylated IRE1 (IRE1α) possesses endoribonuclease activity and excises a 26 base pairs fragment from XBP1 mRNA. XBP1s and XBP1u proteins compete in the activation and inhibition of pro-inflammatory cytokines, respectively. Likewise, dephosphorylation of IRE1α promotes the activation of JUN N-terminal kinase (JNK), which induces apoptosis through the caspase-12 mediated apoptosis pathway [1]

METHODS

Parameters

The mathematical model was constructed from the pathway shown in Figure 1. 10 different species were considered as follows: IRE1, IRE1α, XBP1 mRNA, XBP1s mRNA, XBP1u protein, XBP1s protein, JNK, JNKα, cytokines and apoptosis signal. Additional parameters associated to these species were considered and are summarized in Table 1.

Table 1. Additional parameters considered during the simulation

Parameter	Value	Reference
Length of XBP1	1821 bp	[8]
Protein Transcription rate	2400 bp/min	[9]
Phosphorylation rate of IRE1	0.15 min^{-1}	-
Dephosphorylation rate of IRE1α	0.05 min^{-1}	-
Splicing rate of XBP1	1.25 min^{-1}	[10]
Translation rate of XBP1u	0.495 min^{-1}	[11, 12]
Translation rate of XBP1s	0.5172 min^{-1}	[11, 13]
Cytokine production rate	0.0107 min^{-1}	[14]
Phosphorylation rate of JNK	0.15 min^{-1}	-
Dephosphorylation rate of JNKα	0.05 min^{-1}	-
Apoptosis signal production rate	0.0455 min^{-1}	[15]
Inhibition rate	0.001 min^{-1}	-
mRNA degradation rate	0.0012 min^{-1}	[16]
Protein degradation rate	0.0013 min^{-1}	[17]
Influx of IRE1	0.5 protein/min	-
Influx of JNK	0.15 protein/min	-
Apoptosis signal degradation rate	0.0001 min^{-1}	-
Cytokine degradation rate	0.0001 min^{-1}	-
Initial amount of IRE1	200 nM	-
Initial amount of JNK	400 nM	-

Some of the parameters listed in Table 1 haven't been measured experimentally. These parameters were tuned based on similar parameters found in mammalian cells or what worked better for the dynamics of the model to make sense.

Equations

The dynamics of the model were constructed from the signal pathway shown in Figure 1. The equations used in the mathematical model are as follows:

$$\frac{dIRE1}{dt} = r_p^- IRE\alpha - r_p^+ IRE1 - d_L IRE1 + IN_{IRE1} \quad (1)$$

$$\frac{dIRE1\alpha}{dt} = r_p^+ IRE1 - r_p^- IRE1\alpha - d_L IRE1\alpha \quad (2)$$

$$\frac{dmXBP1}{dt} = r_x IRE1\alpha - d_x mXBP1 - r_s mXBP1 \quad (3)$$

$$\frac{dmXBP1s}{dt} = r_s mXBP1 - d_x mXBP1s \quad (4)$$

$$\frac{dXBP1u}{dt} = r_{Lu} mXBP1 - d_L XBP1u \quad (5)$$

$$\frac{dXBP1s}{dt} = r_{Ls} mXBP1s - d_L XBP1s \quad (6)$$

$$\frac{dJNK}{dt} = r_{JNK}^- JNK\alpha - r_{JNK}^+ JNK\ IRE1\alpha - d_L JNK + IN_{JNK} \quad (7)$$

$$\frac{dJNK\alpha}{dt} = r_{JNK}^+ JNK\ IRE1\alpha - r_{JNK}^- JNK\alpha - d_L JNK\alpha \quad (8)$$

$$\frac{dCyt}{dt} = r_c^+ XBP1s - r_I XBP1u - r_c^- Cyt \quad (9)$$

$$\frac{dApop}{dt} = r_a^+ JNK\alpha - r_a^- Apop \quad (10)$$

The system was assumed to be at steady-state due to the long incubation times in ascites used experimentally by Song et. Al [7].

Computational model

In order to model the effect of the immersion of T lymphocyte in ascites, a computational model in MatLab was employed. To do so, a parameter called *signal* was used to modulate the influence of the ascites. To do so, the value of the phosphorylation and dephosphorylation rate, and the amount of influx of IRE1 and JNK were dependent of the magnitude of the signal as follows:

$$r_p^+ = r_{p0}^+ * \frac{singal}{20} \quad (11)$$

$$r_p^- = r_{p0}^- * \frac{singal}{20} \quad (12)$$

$$IN_{IRE1} = IN_{IRE10} * \frac{singal}{50} \quad (13)$$

$$IN_{JNK} = IN_{JNK0} * \frac{singal}{50} \quad (14)$$

The size of *signal* was correlated with the percentage of ascites arbitrarily as follows: 0% ascites = 0.05 *signal*, 10% ascites = 0.1 *signal* and 100% ascites = 0.15 *signal*.

To determine the influence of each parameter in the expression of XBP1s, each parameter was increased or decreased in one order of magnitude while keeping everything else constant. The effects of up- and down-regulation were determined by comparing the final concentration of XBP1s with that one obtained in the initial model.

RESULTS AND DISCUSSION

Although there is an evident increase in the amount of immunotherapy-based strategies that utilize chimeric antigen receptor (CAR)-T cells for the effective treatment of leukemias, melanomas and lung cancer, these approaches have shown limited to none effects in solid cancers such as ovarian carcinoma [18-20], suggesting that there is an intrinsic immunosuppressive signaling within the tumor microenvironment. Song et al. [7] suggest that tumor-infiltrating immune cells undergo ER stress and activate the UPR in the presence of ascites. The IRE1a-XBP1 pathway was mathematically modelled to further understand their observations. The change in the percentage of XBP1s expression when subjected to ascites is shown in Figure 2. Changes in all the species modelled can be found in Appendix A to J.

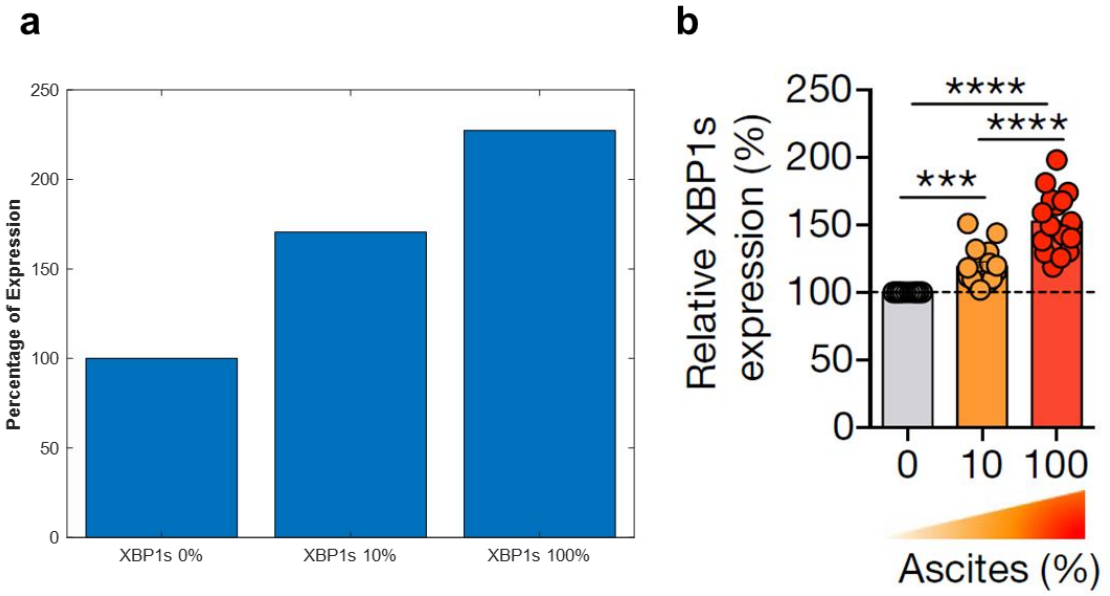

Figure 2. Increase in the relative expression of XBP1s with an increase in the percentage of Ascites. (**a**) Simulation results and (**b**) experimental results. Graph in (**b**) was taken from [7]

As observed in Figure 1, the modelled expression of XBP1s in T cells after being subjected to different concentrations of ascites behaves closely to that observed experimentally. Interestingly, the percentage change in the amount of IREIα, XBP1 mRNA, XBP1s mRNA, XBP1u and cytokines was the same as that of XBP1s, suggesting that all these species are tightly related. Similarly, the change in apoptotic signal was tightly related with that one in JNKα. These confirms that the model was correctly constructed from that shown in Figure 1.

Nonetheless, the question on what should be altered to better modulate the activation of the UPR within the tumor microenvironment remains unanswered. To understand this better, the sensitivity on the expression of XBP1s at a constant exposure to ascites towards a variation on the parameters included in the model was measured. A qualitative behavior is recorded in Table 2 and the exact changes in concentration can be found in Appendix K to CC.

Table 2. Effect of one order of magnitude increase or decrease of each parameter on the expression of XBP1s

Parameter	Increase	Decrease
Length of XBP1 [bp]	---	+++
Protein Transcription rate [bp/min]	+++	--
Phosphorylation rate of IRE1 [1/min]	++	-
Dephosphorylation rate of IRE1α [1/min]	-	+
Splicing rate of XBP1 [1/min]	0	0
Translation rate of XBP1u [1/min]	0	0
Translation rate of XBP1s [1/min]	+++	--
Cytokine production rate [1/min]	0	0
Phosphorylation rate of JNK [1/min]	0	0
Dephosphorylation rate of JNKα [1/min]	0	0
Apoptosis signal production rate [1/min]	0	0
Inhibition rate [1/min]	0	0
mRNA degradation rate [1/min]	--	+++
Protein degradation rate [1/min]	--	+++
Influx of IRE1 [protein/min]	+++	--

Influx of JNK [protein/min]	0	0
Apoptosis signal degradation rate [1/min]	0	0
Cytokine degradation rate [1/min]	0	0
Initial amount of IRE1 [nM]	0	0
Initial amount of JNK [nM]	0	0

According to the results, only the length of XBP1, the protein transcription rate, the phosphorylation rate of IRE1, the dephosphorylation rate of IRE1, the translation rate of XBP1s, the mRNA degradation rate, the protein degradation rate and the influx of IRE1, seem to have an effect on the expression of XBP1s when varying them in one order of magnitude. Notice that, among these parameters, only the influx of IRE1 can be changed without altering side mechanisms and pathways within the cell.

According to the model, decreasing the influx of IRE1 by one order of magnitude reduces the expression of XBP1s by 90%, whereas increasing it by the same amount raises the expression of XBP1s in an 8-fold. These results suggest that silencing the IRE1 gene in CAR-T cells could improve their effectiveness in immunotherapies against solid cancers.

CONCLUSION

The mathematical model described here coupled with the experimental data collected by Song et al. [7] indicate that activation of the IREα-XBP1 pathway within the URP in tumor-infiltrating T cells decreases their ability to control invasion. The proposed model shows a comparable behavior to that found experimentally and provides a platform to test the effect of changes in different cellular parameters involved in the process. From this analysis it can be proposed that disruption of the IREα-XBP1 pathway by inhibition of the synthesis of new IRE1 can alleviate the effect of glucose deprivation within the tumor microenvironment and enhance the cytotoxic effect of synthetic or natural T lymphocytes.

ACKNOWLEDGEMENTS

I would like to thank Dr. Mathew Paszek and Dr. Jeffrey Varner for their feedback during the presentation of this project which serve as a baseline for the discussion presented in this report.

REFERENCES

[1] D. J. Todd, A. H. Lee, and L. H. Glimcher, "The endoplasmic reticulum stress response in immunity and autoimmunity," *Nat Rev Immunol,* vol. 8, no. 9, pp. 663-74, Sep 2008.

[2] K. J. Travers, C. K. Patil, L. Wodicka, D. J. Lockhart, J. S. Weissman, and P. Walter, "Functional and genomic analyses reveal an essential coordination between the unfolded protein response and ER-associated degradation," *Cell,* vol. 101, no. 3, pp. 249-58, Apr 28 2000.
[3] H. P. Harding, Y. Zhang, and D. Ron, "Protein translation and folding are coupled by an endoplasmic-reticulum-resident kinase," *Nature,* vol. 397, no. 6716, pp. 271-4, Jan 21 1999.
[4] K. Haze, H. Yoshida, H. Yanagi, T. Yura, and K. Mori, "Mammalian transcription factor ATF6 is synthesized as a transmembrane protein and activated by proteolysis in response to endoplasmic reticulum stress," *Mol Biol Cell,* vol. 10, no. 11, pp. 3787-99, Nov 1999.
[5] N. N. Pavlova and C. B. Thompson, "The Emerging Hallmarks of Cancer Metabolism," *Cell Metab,* vol. 23, no. 1, pp. 27-47, Jan 12 2016.
[6] X. Sun *et al.*, "Deletion of the pH sensor GPR4 decreases renal acid excretion," *J Am Soc Nephrol,* vol. 21, no. 10, pp. 1745-55, Oct 2010.
[7] M. Song *et al.*, "IRE1alpha-XBP1 controls T cell function in ovarian cancer by regulating mitochondrial activity," *Nature,* vol. 562, no. 7727, pp. 423-428, Oct 2018.
[8] I. Unlu, Y. Lu, and X. Wang, "The cyclic phosphodiesterase CNP and RNA cyclase RtcA fine-tune noncanonical XBP1 splicing during ER stress," *J Biol Chem,* vol. 293, no. 50, pp. 19365-19376, Dec 14 2018.
[9] D. A. Jackson, A. Pombo, and F. Iborra, "The balance sheet for transcription: an analysis of nuclear RNA metabolism in mammalian cells," *FASEB J,* vol. 14, no. 2, pp. 242-54, Feb 2000.
[10] A. Audibert, D. Weil, and F. Dautry, "In vivo kinetics of mRNA splicing and transport in mammalian cells," *Mol Cell Biol,* vol. 22, no. 19, pp. 6706-18, Oct 2002.
[11] S. O. Olofsson *et al.*, "Structure and biosynthesis of apolipoprotein B," *Am Heart J,* vol. 113, no. 2 Pt 2, pp. 446-52, Feb 1987.
[12] H. C. Liou *et al.*, "An Hla-Dr-Alpha-Promoter DNA-Binding Protein Is Expressed Ubiquitously and Maps to Human Chromosome-22 and Chromosome-5," (in English), *Immunogenetics,* vol. 34, no. 5, pp. 286-292, Nov 1991.
[13] D. Martin *et al.*, "Unspliced X-box-binding Protein 1 (XBP1) Protects Endothelial Cells from Oxidative Stress through Interaction with Histone Deacetylase 3," (in English), *Journal of Biological Chemistry,* vol. 289, no. 44, pp. 30625-30634, Oct 31 2014.
[14] A. Bas, G. Forsberg, S. Hammarstrom, and M. L. Hammarstrom, "Utility of the housekeeping genes 18S rRNA, beta-actin and glyceraldehyde-3-phosphate-dehydrogenase for normalization in real-time quantitative reverse transcriptase-polymerase chain reaction analysis of gene expression in human T lymphocytes," (in English), *Scandinavian Journal of Immunology,* vol. 59, no. 6, pp. 566-573, Jun 2004.
[15] J. G. Albeck, J. M. Burke, S. L. Spencer, D. A. Lauffenburger, and P. K. Sorger, "Modeling a Snap-Action, Variable-Delay Switch Controlling Extrinsic Cell Death," (in English), *Plos Biology,* vol. 6, no. 12, pp. 2831-2852, Dec 2008.
[16] E. Yang *et al.*, "Decay rates of human mRNAs: Correlation with functional characteristics and sequence attributes," (in English), *Genome Research,* vol. 13, no. 8, pp. 1863-1872, Aug 2003.
[17] M. K. Doherty, D. E. Hammond, M. J. Clagule, S. J. Gaskell, and R. J. Beynon, "Turnover of the Human Proteome: Determination of Protein Intracellular Stability by Dynamic SILAC," (in English), *Journal of Proteome Research,* vol. 8, no. 1, pp. 104-112, Jan 2009.
[18] A. Gadducci and M. E. Guerrieri, "Immune Checkpoint Inhibitors in Gynecological Cancers: Update of Literature and Perspectives of Clinical Research," (in English), *Anticancer Research,* vol. 37, no. 11, pp. 5955-5965, Nov 2017.

[19] V. Jindal, E. Arora, S. Gupta, A. Lal, M. Masab, and R. Potdar, "Prospects of chimeric antigen receptor T cell therapy in ovarian cancer," (in English), *Medical Oncology,* vol. 35, no. 5, May 2018.
[20] L. E. Kandalaft *et al.*, "Autologous lysate-pulsed dendritic cell vaccination followed by adoptive transfer of vaccine-primed ex vivo co-stimulated T cells in recurrent ovarian cancer," (in English), *Oncoimmunology,* vol. 2, no. 1, Jan 2013.

APPENDIX

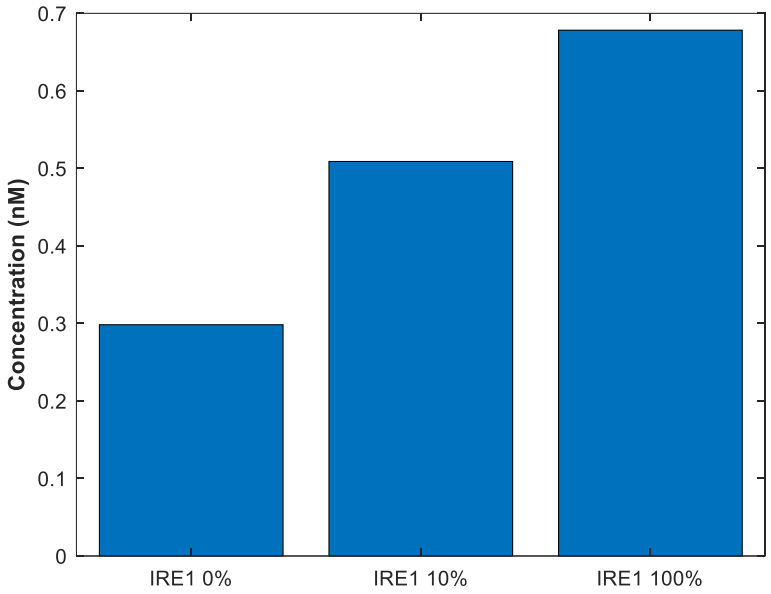

Appendix A. Change in the concentration of IRE1 in T lymphocytes when subjected to 0%, 10% and 100% of ascites.

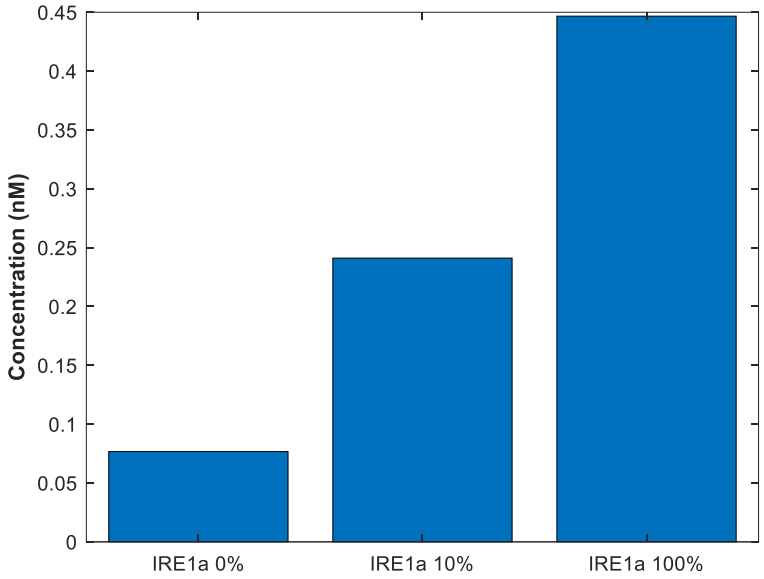

Appendix B. Change in the concentration of IRE1α in T lymphocytes when subjected to 0%, 10% and 100% of ascites.

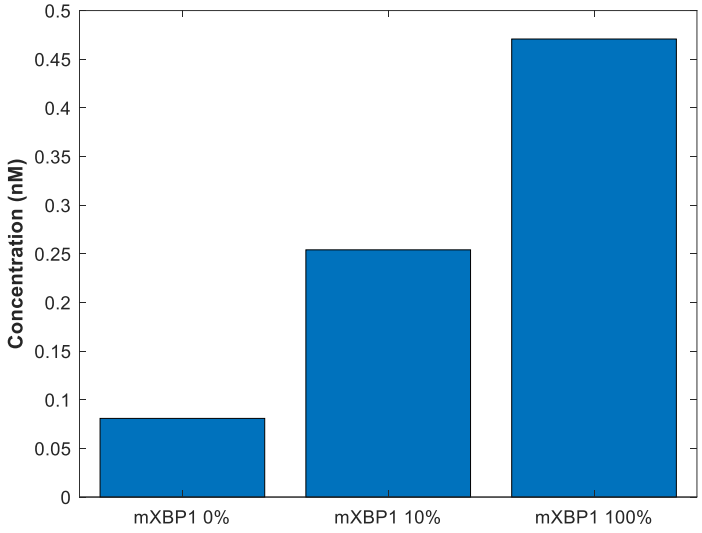

Appendix C. Change in the concentration of XBP1 mRNA in T lymphocytes when subjected to 0%, 10% and 100% of ascites.

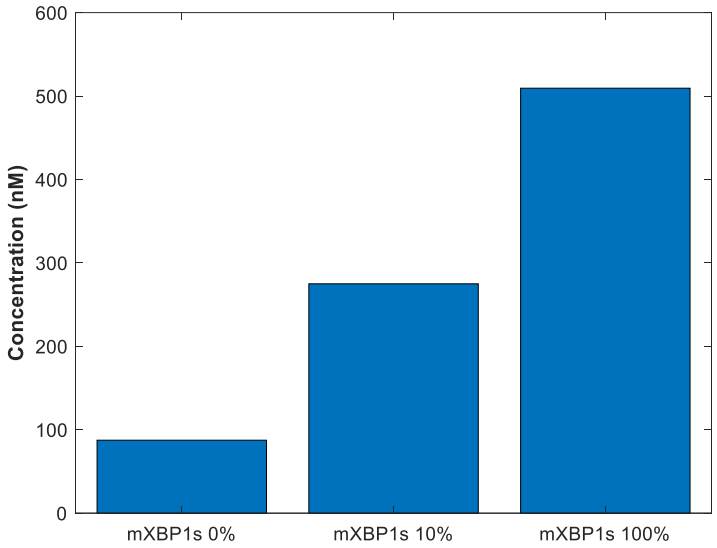

Appendix D. Change in the concentration of spliced XBP1 (XBP1s) mRNA in T lymphocytes when subjected to 0%, 10% and 100% of ascites.

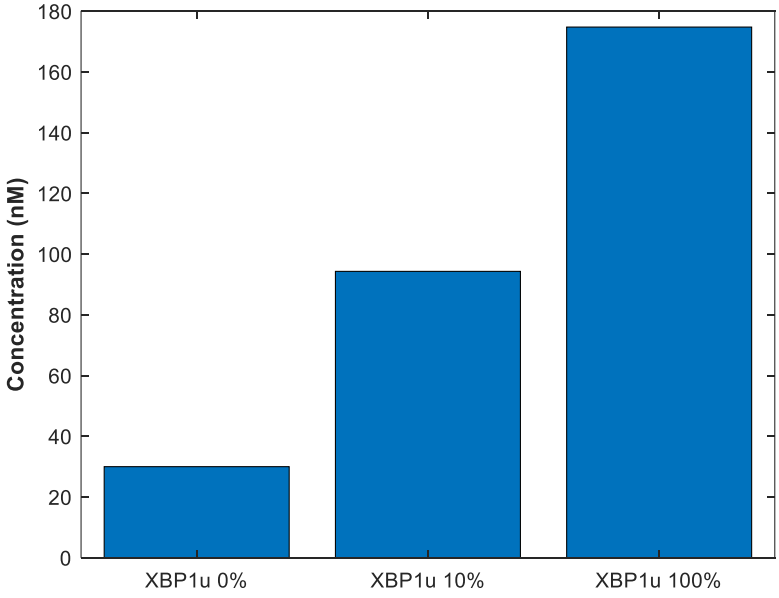

Appendix E. Change in the concentration of unspliced XBP1 (XBP1u) in T lymphocytes when subjected to 0%, 10% and 100% of ascites.

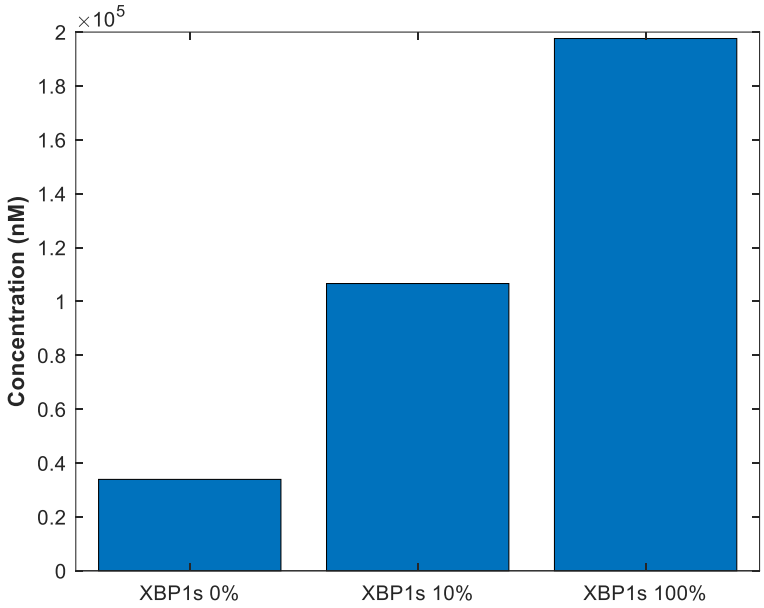

Appendix F. Change in the concentration of spliced XBP1 (XBP1s) in T lymphocytes when subjected to 0%, 10% and 100% of ascites.

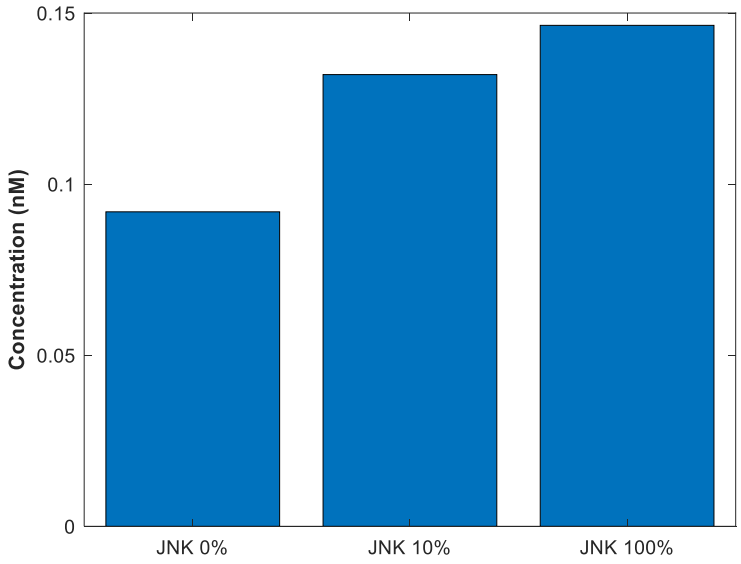

Appendix G. Change in the concentration of JUN N-terminal kinase (JNK) in T lymphocytes when subjected to 0%, 10% and 100% of ascites.

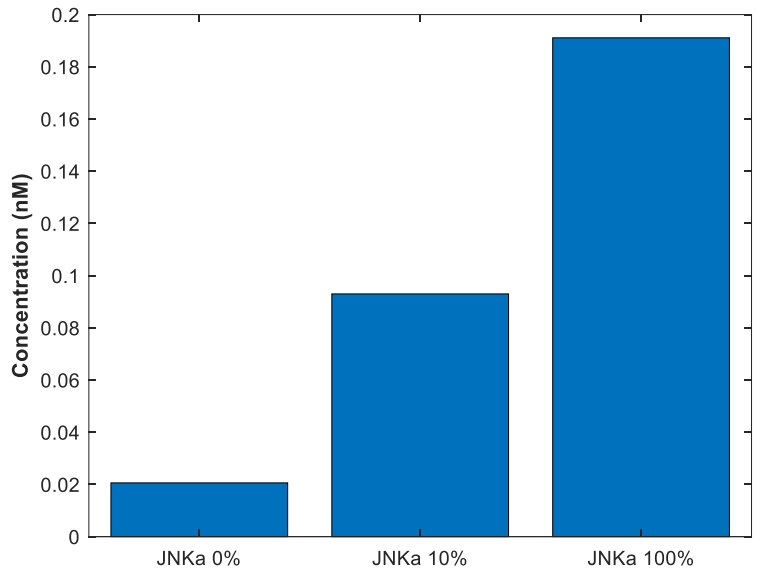

Appendix H. Change in the concentration of active JUN N-terminal kinase (JNKα) in T lymphocytes when subjected to 0%, 10% and 100% of ascites.

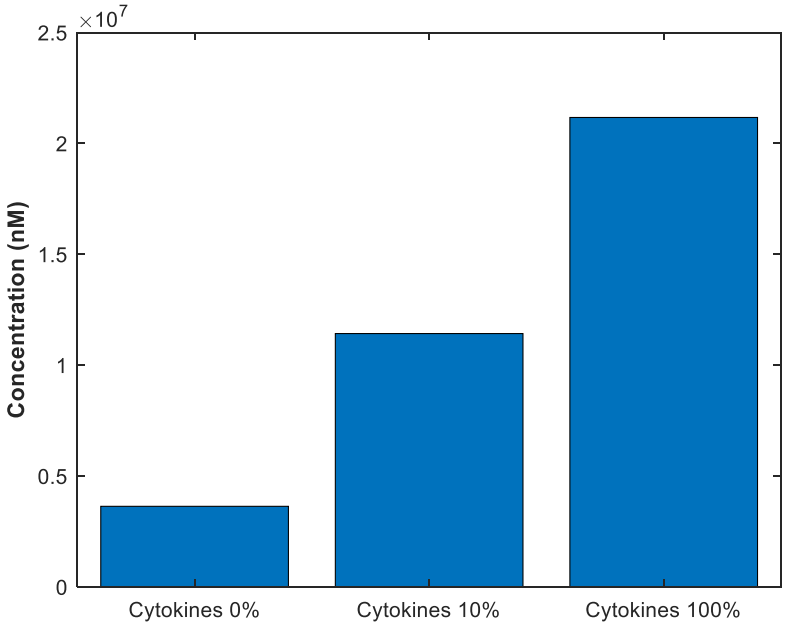

Appendix I. Change in the concentration of cytokines produced by T lymphocytes when subjected to 0%, 10% and 100% of ascites.

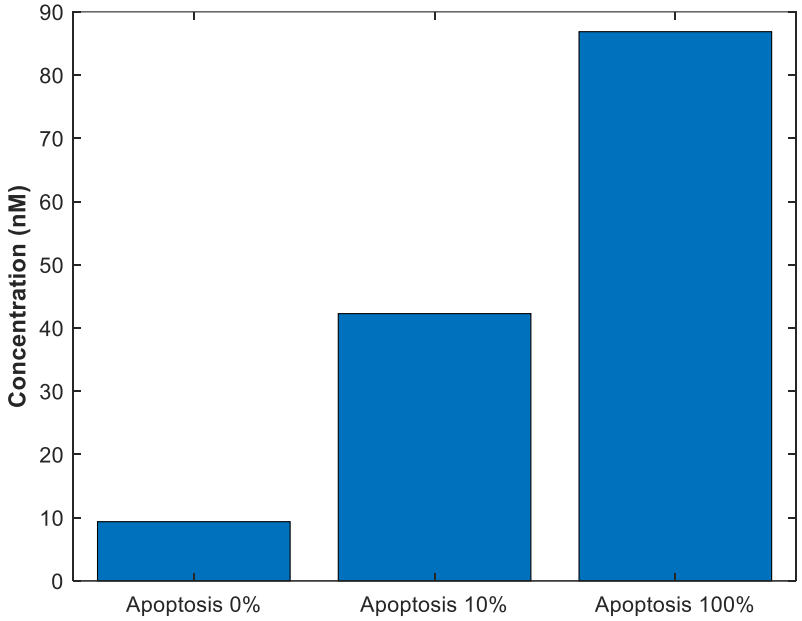

Appendix J. Change in the concentration of apoptotic signal in T lymphocytes when subjected to 0%, 10% and 100% of ascites.

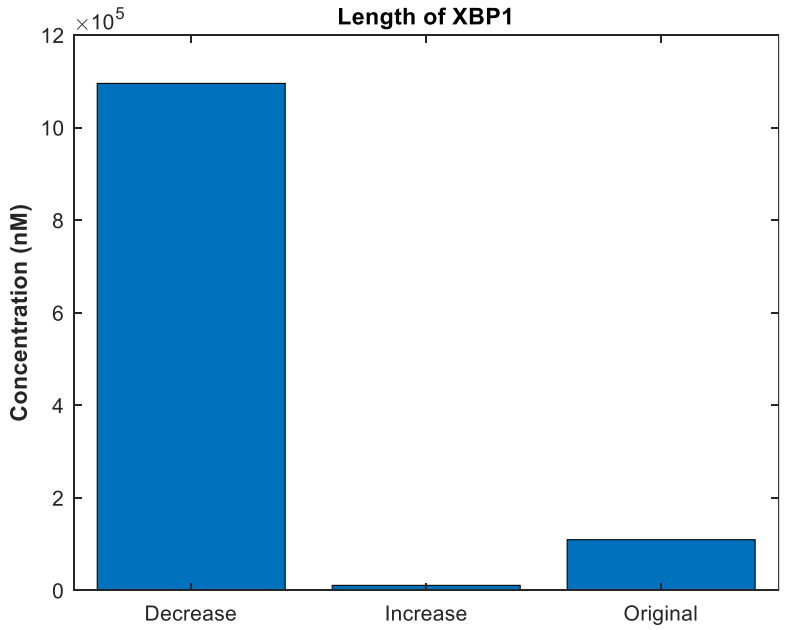

Appendix K. Changes in XBP1s concentration when decreasing or increasing the length of XBP1 gene in 10% ascites

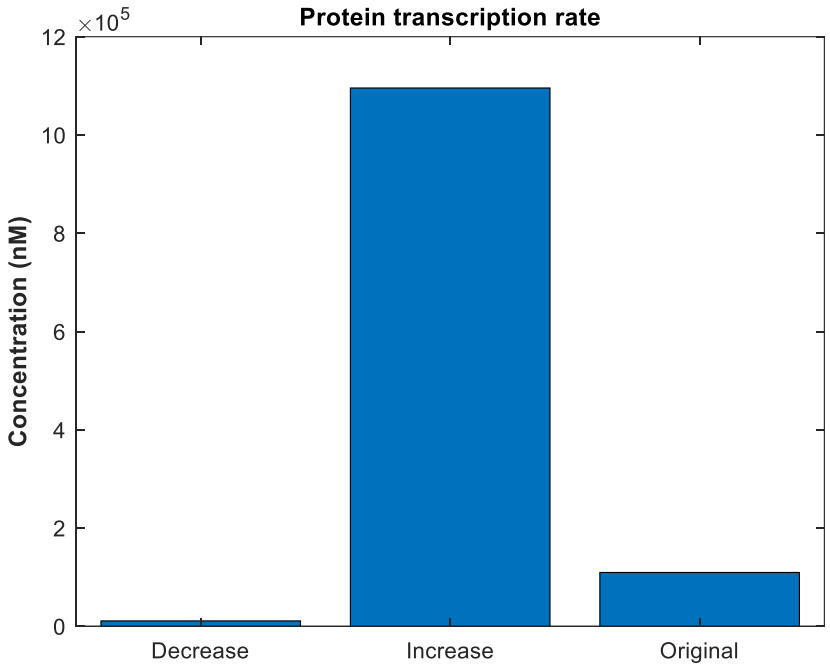

Appendix L. Changes in XBP1s concentration when decreasing or increasing the protein transcription rate in 10% ascites

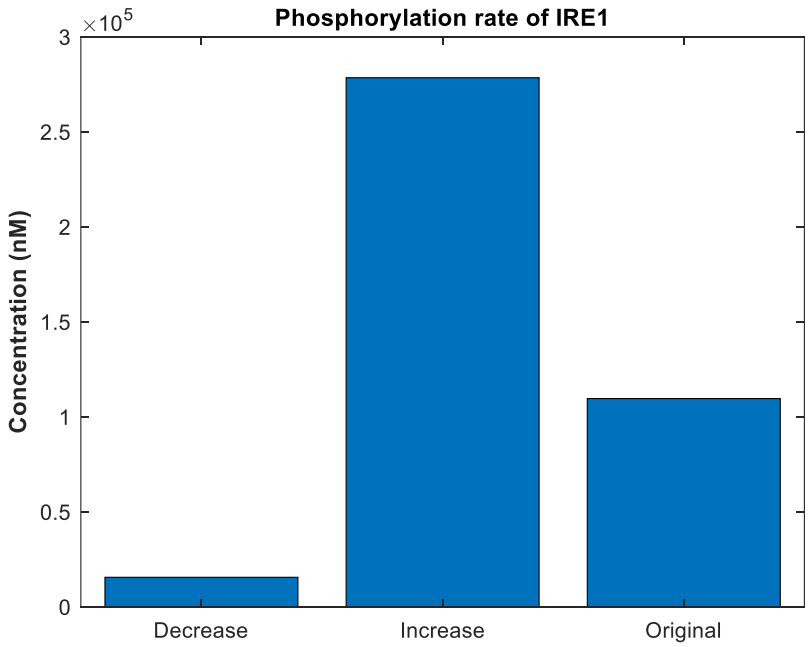

Appendix M. Changes in XBP1s concentration when decreasing or increasing the phosphorylation rate of IRE1 in 10% ascites

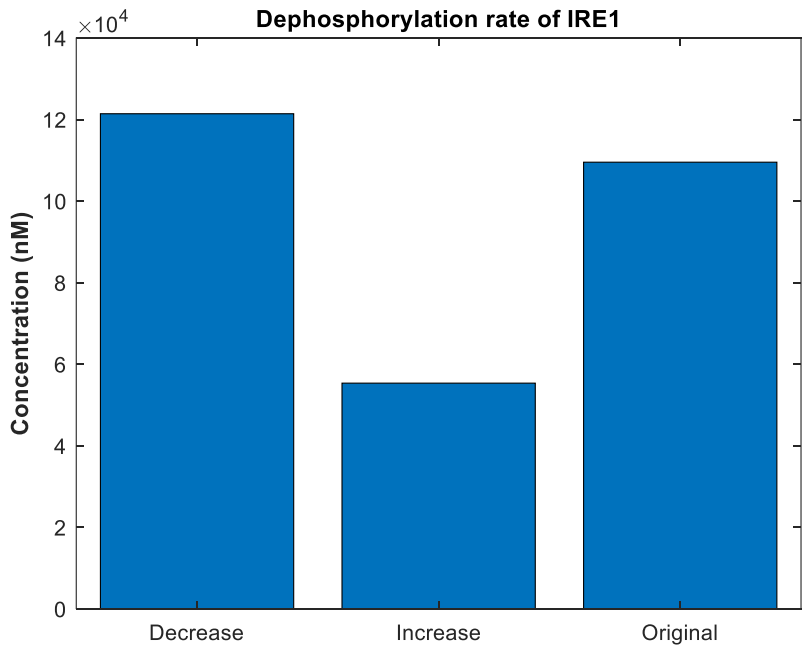

Appendix N. Changes in XBP1s concentration when decreasing or increasing the dephosphorylation rate of IRE1 in 10% ascites

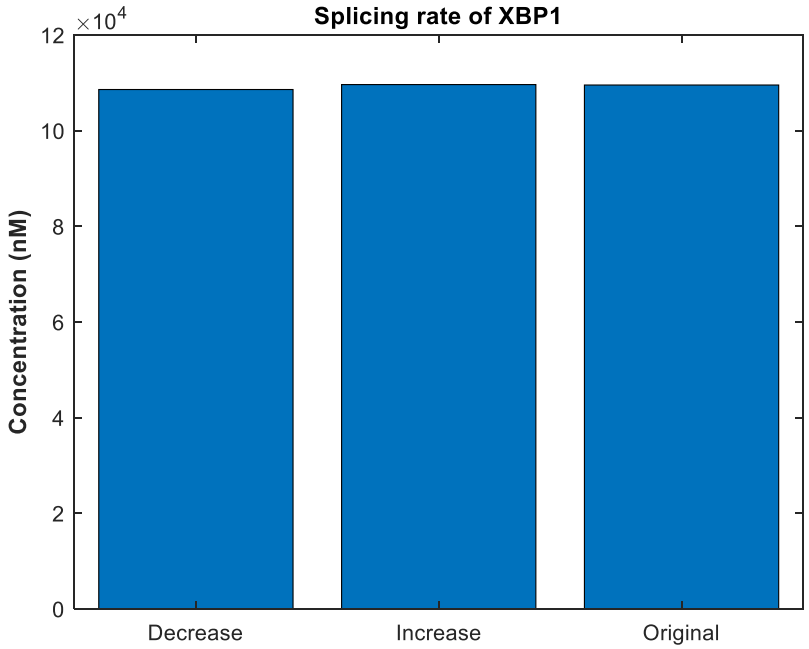

Appendix O. Changes in XBP1s concentration when decreasing or increasing the splicing rate of XBP1 in 10% ascites

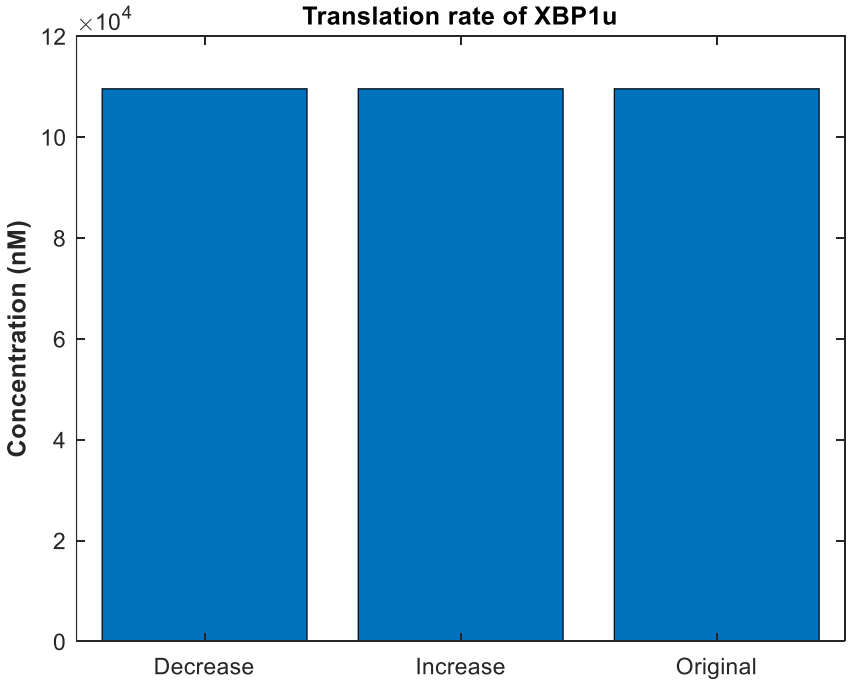

Appendix P. Changes in XBP1s concentration when decreasing or increasing the translation rate of XBP1u in 10% ascites

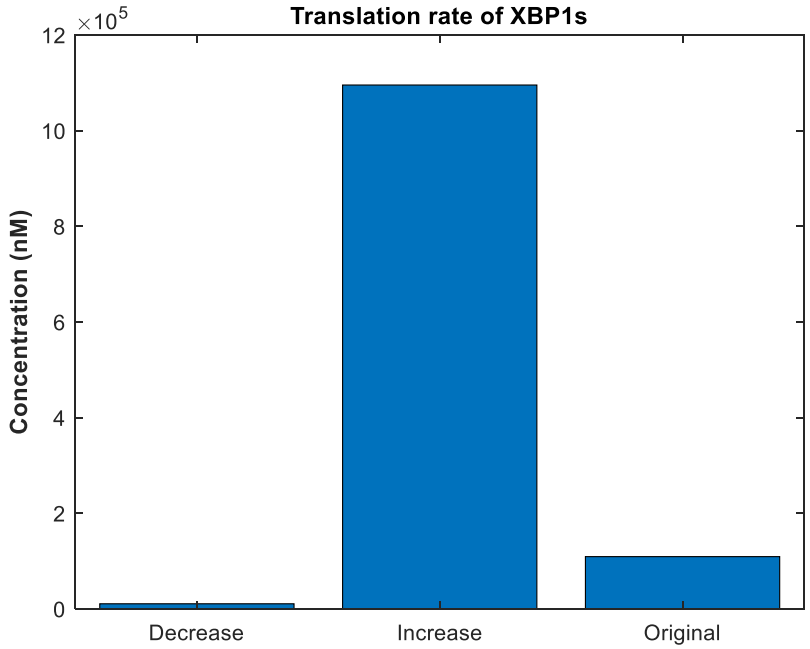

Appendix Q. Changes in XBP1s concentration when decreasing or increasing the translation rate of XBP1s in 10% ascites

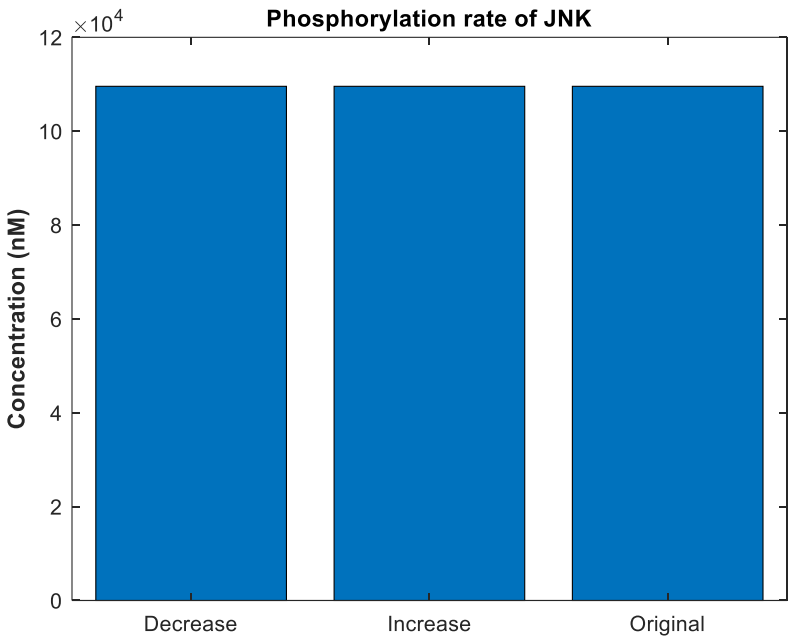

Appendix R. Changes in XBP1s concentration when decreasing or increasing the phosphorylation rate of JNK in 10% ascites

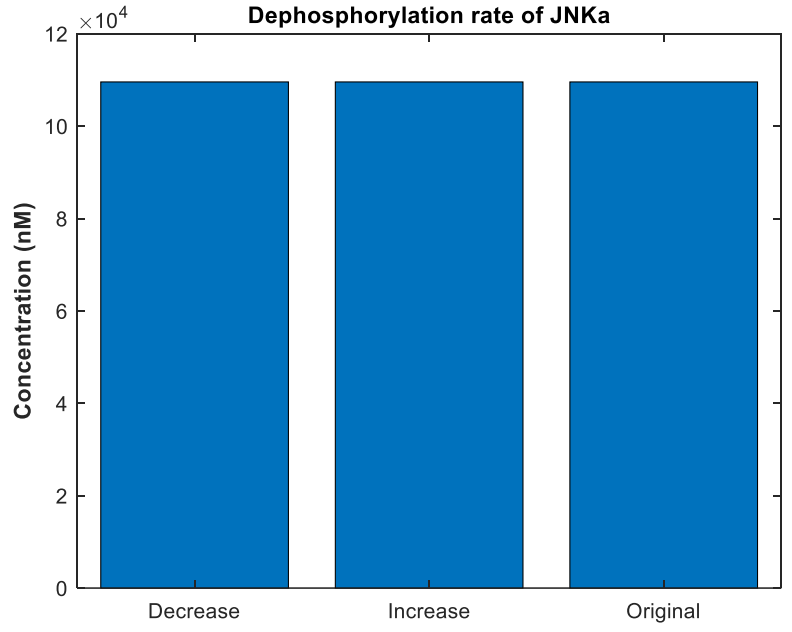

Appendix S. Changes in XBP1s concentration when decreasing or increasing the dephosphorylation rate of JNK in 10% ascites

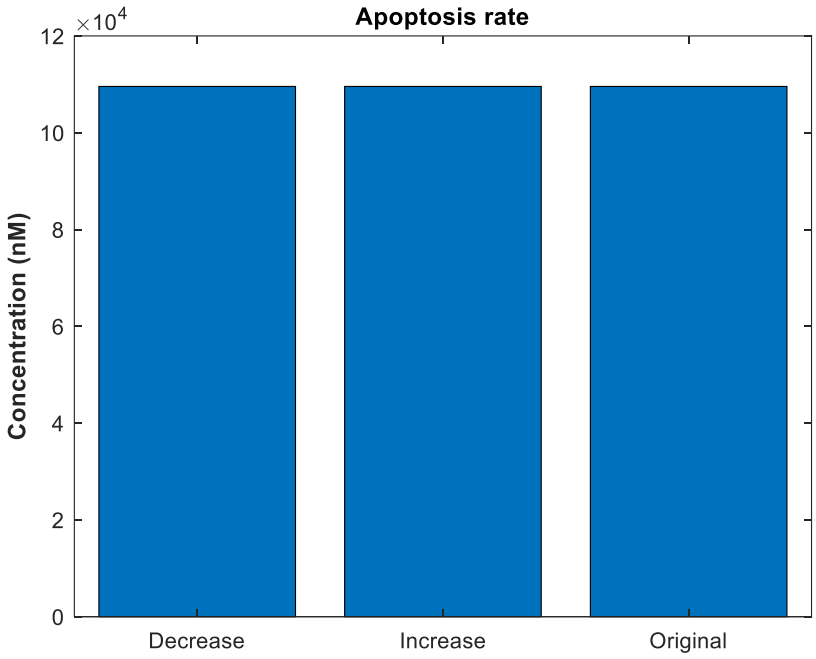

Appendix T. Changes in XBP1s concentration when decreasing or increasing the apoptosis rate in 10% ascites

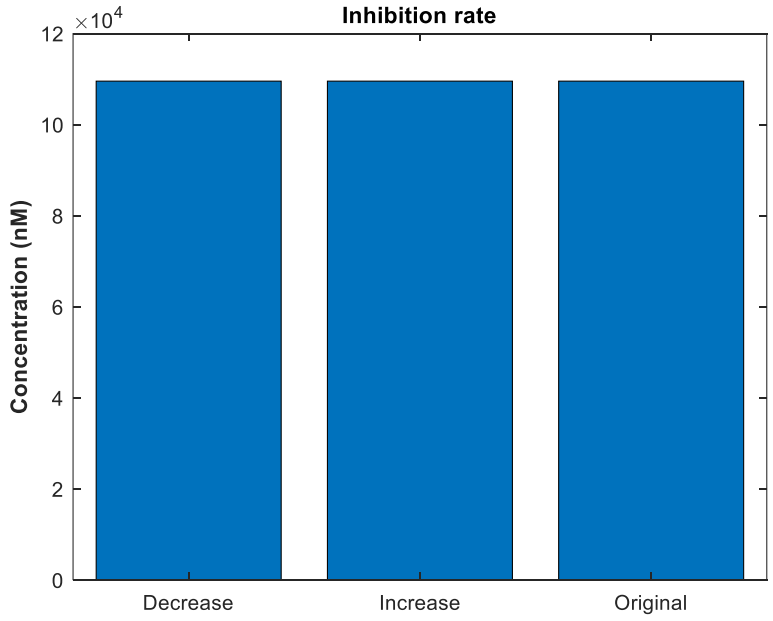

Appendix U. Changes in XBP1s concentration when decreasing or increasing the inhibition rate in 10% ascites

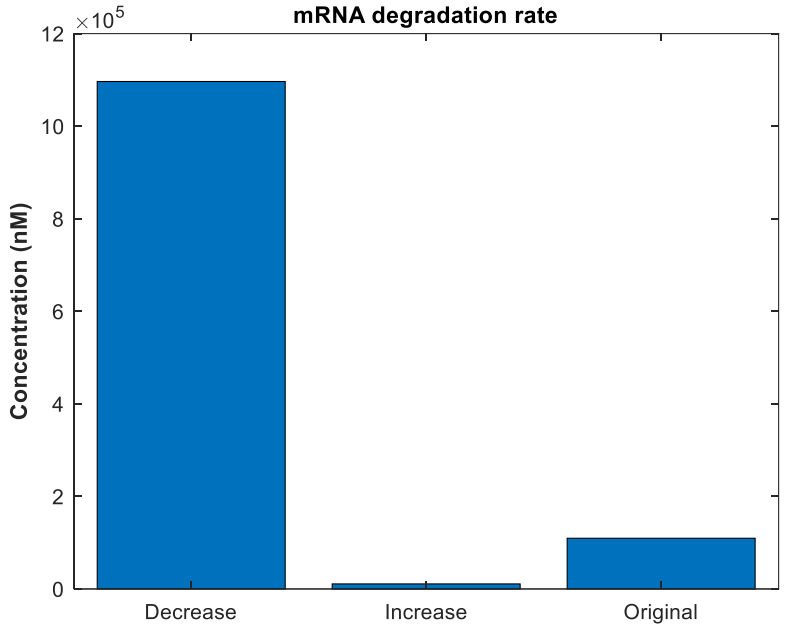

Appendix V. Changes in XBP1s concentration when decreasing or increasing the mRNA degradation rate in 10% ascites

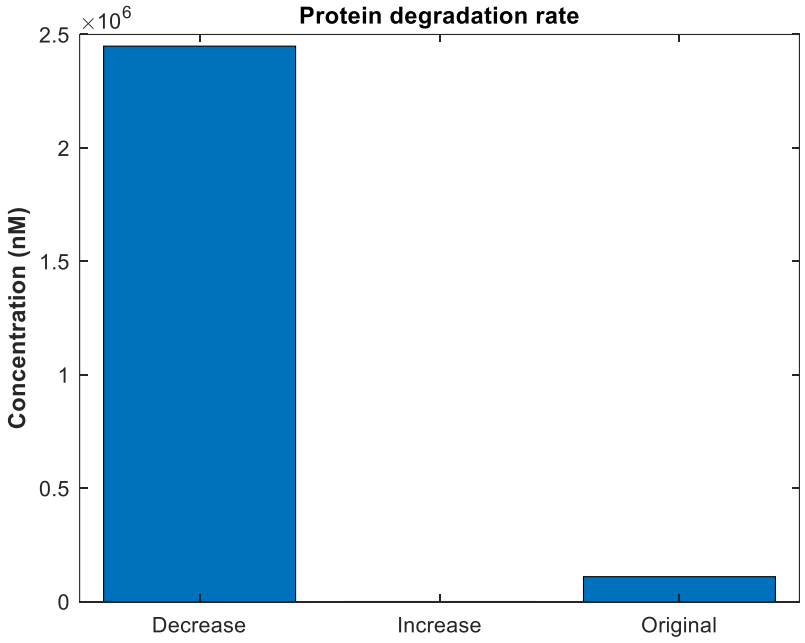

Appendix W. Changes in XBP1s concentration when decreasing or increasing the protein degradation rate in 10% ascites

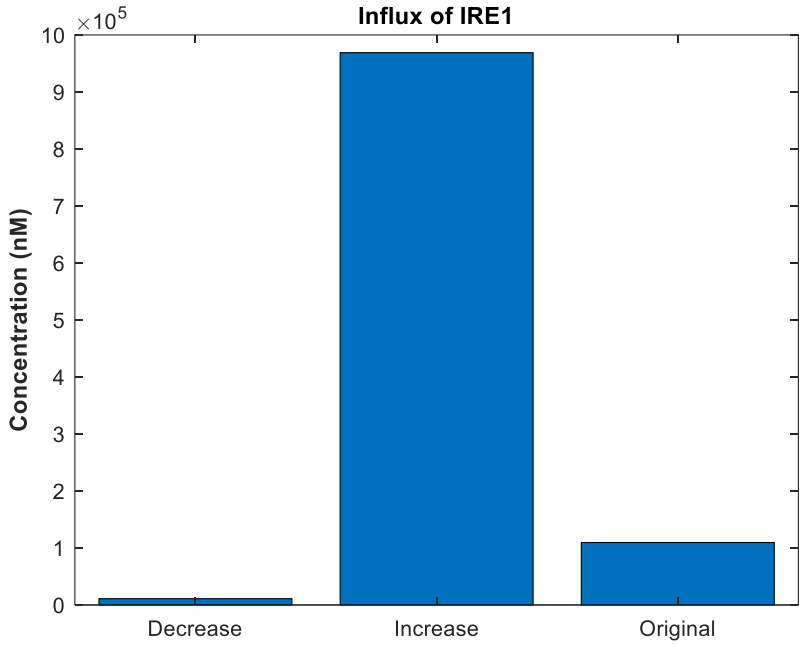

Appendix X. Changes in XBP1s concentration when decreasing or increasing the influx of IRE1 in 10% ascites

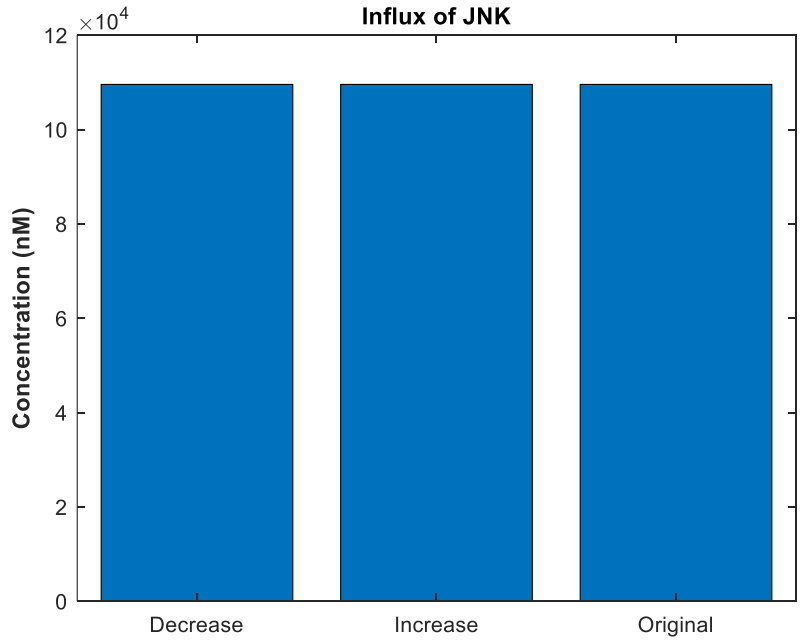

Appendix Y. Changes in XBP1s concentration when decreasing or increasing the influx of JNK in 10% ascites

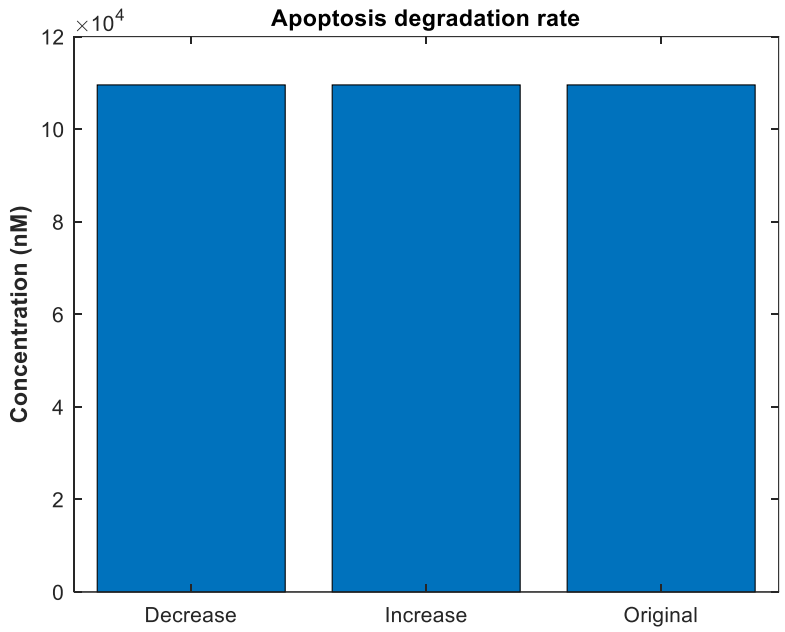

Appendix Z. Changes in XBP1s concentration when decreasing or increasing the apoptosis degradation rate in 10% ascites

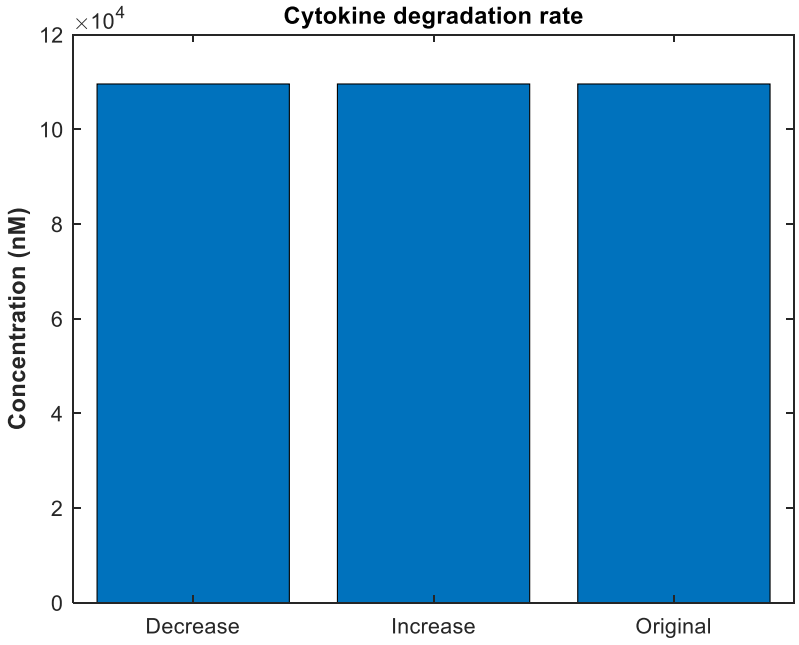

Appendix AA. Changes in XBP1s concentration when decreasing or increasing the cytokine degradation rate in 10% ascites

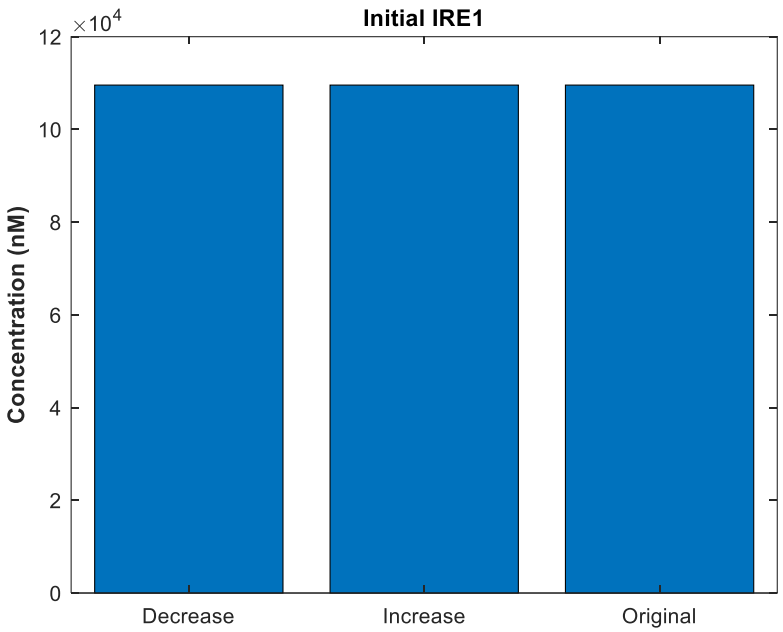

Appendix BB. Changes in XBP1s concentration when decreasing or increasing the initial concentration of IRE1 in 10% ascites

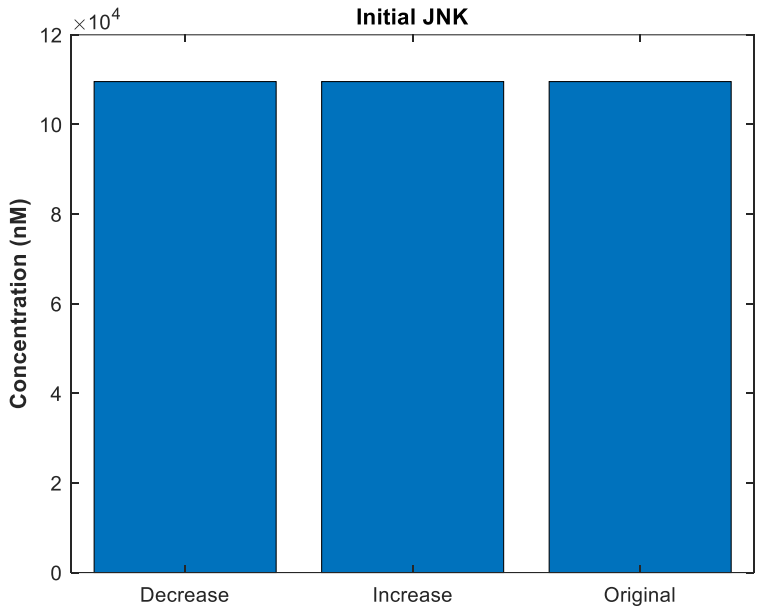

Appendix CC. Changes in XBP1s concentration when decreasing or increasing the initial concentration of JNK in 10% ascites

THE CODE:

```
%% Final Project - Natalia Lopez-Barbosa
%close all;
%clear all;
clc;

%Parameters

global rx rpp rpm rs rlu rls rc rjnkp rjnkm ra ri dx dl INi INj
ram rcm signal x0 x

Lx = 1820; %Length of XBP1 from
https://www.ncbi.nlm.nih.gov/nuccore/NM_005080
Rx = 2400; %[bp/min] Transcription rate in humans from
Bionumbers
rx = Rx/Lx; %Transcription rate of XBP1
rpp = 0.15; %[1/min]Phosphorylation rate of IRE1
rpm = 0.05; %[1/min] Dephosphorylation rate of IRE1a
rs = 1/0.8; %[1/min] Splicing rate of XBP1 bionumbers
rlu = (5/606)*60; %[1/min] Translation rate of XBP1u bionumbers
rls = (5/580)*60; %[1/min] Translation rate of XBP1s bionumbers
rc = (4.5/7)/60; %[1/min] Cytokine production rate bionumbers
rjnkp = 0.15; %[1/min] Phosphorylation rate of JNK
rjnkm = 0.05; %[1/min] Dephosphorylation rate of JNKa
ra = 1/22; %[1/min] Estimated from parameters in Bionumbers
ri = 0.001; %[1/min] inhibition rate
dx = log(2)/(10*60); %[1/min] mRNA degradation rate from
Bionumbers
dl = 0.08/60; %[1/min] protein degradation rate from bionumbers
INi = 0.5; %[protein/min] Influx of IRE1
INj = 0.15; %[protein/min] Influx of JNK
ram = 0.0001;
rcm = 0.0001;

rpp = rpp*signal/20;
rpm = rpm*signal/20;
INi = INi*signal/50;
INj = INj*signal/50;


%Steady-state: at the kinetic limit

fun = @steady;
x = fsolve(fun,x0);


function F = steady(x)
```

```
global rx rpp rpm rs rlu rls rc rjnkp rjnkm ra ri dx dl INi INj
ram rcm

F(1) = rpm*x(2)-rpp*x(1)-dl*x(1)+INi;
F(2) = rpp*x(1)-rpm*x(2)-dl*x(2);
F(3) = rx*x(2)-dx*x(3)-rs*x(3);
F(4) = rs*x(3)-dx*x(4);
F(5) = rlu*x(3)-dl*x(5);
F(6) = rls*x(4)-dl*x(6);
F(7) = INj+rjnkm*x(8)-rjnkp*x(7)*x(2)-dl*x(7);
F(8) = rjnkp*x(7)*x(2)-rjnkm*x(8)-dl*x(8);
F(9) = rc*x(6)-ri*x(5)-rcm*x(9);
F(10) = ra*x(8)-ram*x(10);


%% Building conditions
close all;
clear all;
clc;

global signal x0 x

signal = 0.05; %Signaling ER stress

%Initial conditions

x0 = zeros(1,10);
x0(1,1) = 200; %IRE1
x0(1,2) = 0; %IRE1a
x0(1,3) = 0; %mXBP1
x0(1,4) = 0; %mXBP1s
x0(1,5) = 0; %XBP1u
x0(1,6) = 0; %XBP1s
x0(1,7) = 400; %JNK
x0(1,8) = 0; %JNKa
x0(1,9) = 0; %Cytokines
x0(1,10) = 0; %Apoptotic signal
main;
y(:,1) = x.';

j=2;
for i=0.1:0.05:0.15
    signal = i;
    x0(1,1) = 180+(i*(1.2-i));
    main;
    y(:,j) = x.';
```

```
    j = j+1;
end

z = y(:,:)./y(:,1);
z = z.*100;

%% Raw Figures
figure(1)
%xla =
categorical({'IRE1','IRE1a','mXBP1','mXBP1s','XBP1u','XBP1s','JN
K','JNKa','Cytokines','Apoptosis'});
xla = categorical({'IRE1 0%','IRE1 10%','IRE1 100%'});
xla = reordercats(xla,{'IRE1 0%','IRE1 10%','IRE1 100%'});
bar(xla,y(1,:))
ylabel('Concentration (nM)','FontWeight','Bold');
% ylim([90 380])

figure(2)
xla = categorical({'IRE1a 0%','IRE1a 10%','IRE1a 100%'});
xla = reordercats(xla,{'IRE1a 0%','IRE1a 10%','IRE1a 100%'});
bar(xla,y(2,:))
ylabel('Concentration (nM)','FontWeight','Bold');
% ylim([0 285])

figure(3)
xla = categorical({'mXBP1 0%','mXBP1 10%','mXBP1 100%'});
xla = reordercats(xla,{'mXBP1 0%','mXBP1 10%','mXBP1 100%'});
bar(xla,y(3,:))
ylabel('Concentration (nM)','FontWeight','Bold');
% ylim([0 300])

figure(4)
xla = categorical({'mXBP1s 0%','mXBP1s 10%','mXBP1s 100%'});
xla = reordercats(xla,{'mXBP1s 0%','mXBP1s 10%','mXBP1s 100%'});
bar(xla,y(4,:))
ylabel('Concentration (nM)','FontWeight','Bold');
% ylim([316000 321000])

figure(5)
xla = categorical({'XBP1u 0%','XBP1u 10%','XBP1u 100%'});
xla = reordercats(xla,{'XBP1u 0%','XBP1u 10%','XBP1u 100%'});
bar(xla,y(5,:))
ylabel('Concentration (nM)','FontWeight','Bold');
% ylim([108000 110100])

figure(6)
xla = categorical({'XBP1s 0%','XBP1s 10%','XBP1s 100%'});
```

```
xla = reordercats(xla,{'XBP1s 0%','XBP1s 10%','XBP1s 100%'});
bar(xla,y(6,:))
ylabel('Concentration (nM)','FontWeight','Bold');
% ylim([122000000 124500000])

figure(7)
xla = categorical({'JNK 0%','JNK 10%','JNK 100%'});
xla = reordercats(xla,{'JNK 0%','JNK 10%','JNK 100%'});
bar(xla,y(7,:))
ylabel('Concentration (nM)','FontWeight','Bold');
% ylim([0 115])

figure(8)
xla = categorical({'JNKa 0%','JNKa 10%','JNKa 100%'});
xla = reordercats(xla,{'JNKa 0%','JNKa 10%','JNKa 100%'});
bar(xla,y(8,:))
ylabel('Concentration (nM)','FontWeight','Bold');
% ylim([112.36 112.365])

figure(9)
xla = categorical({'Cytokines 0%','Cytokines 10%','Cytokines
100%'});
xla = reordercats(xla,{'Cytokines 0%','Cytokines 10%','Cytokines
100%'});
bar(xla,y(9,:))
ylabel('Concentration (nM)','FontWeight','Bold');
% ylim([13150000000 13330000000])

figure(10)
xla = categorical({'Apoptosis 0%','Apoptosis 10%','Apoptosis
100%'});
xla = reordercats(xla,{'Apoptosis 0%','Apoptosis 10%','Apoptosis
100%'});
bar(xla,y(10,:))
ylabel('Concentration (nM)','FontWeight','Bold');
% ylim([51073.2 51074.3])

%% Percentage Figures

figure(11)
xla = categorical({'XBP1s 0%','XBP1s 10%','XBP1s 100%'});
xla = reordercats(xla,{'XBP1s 0%','XBP1s 10%','XBP1s 100%'});
bar(xla,z(1,:))
ylabel('Percentage of Expression','FontWeight','Bold');

%% Parameters sensitivity
close all;
```

```
clear all;
clc;

global rx rpp rpm rs rlu rls rc rjnkp rjnkm ra ri dx dl INi INj
ram rcm signal x0 x

x0 = zeros(1,10);
x0(1,1) = 200; %IRE1
x0(1,2) = 0; %IRE1a
x0(1,3) = 0; %mXBP1
x0(1,4) = 0; %mXBP1s
x0(1,5) = 0; %XBP1u
x0(1,6) = 0; %XBP1s
x0(1,7) = 400; %JNK
x0(1,8) = 0; %JNKa
x0(1,9) = 0; %Cytokines
x0(1,10) = 0; %Apoptotic signal

signal = 0.1;

Par = [1820 2400 0.15 0.05 1.25 0.495 0.5172 0.0107 0.15 0.05
0.0455 0.001 0.0012 0.0013 0.5 0.15 0.0001 0.0001 200 400];
name = ["Length of XBP1","Protein transcription
rate","Phosphorylation rate of IRE1","Dephosphorylation rate of
IRE1",...
    "Splicing rate of XBP1","Translation rate of
XBP1u","Translation rate of XBP1s",...
    "Cytokine production rate","Phosphorylation rate of
JNK","Dephosphorylation rate of JNKa",...
    "Apoptosis rate","Inhibition rate","mRNA degradation
rate","Protein degradation rate",...
    "Influx of IRE1","Influx of JNK","Apoptosis degradation
rate","Cytokine degradation rate",...
    "Initial IRE1", "Initial JNK"];

%Loops are fun
for i=1:20
    %Before changing things
    tempPar = Par(1,i);
    rx = Par(1,2)/Par(1,1); %Transcription rate of XBP1
    rpp = Par(1,3); %[1/min]Phosphorylation rate of IRE1
    rpm = Par(1,4); %[1/min] Dephosphorylation rate of IRE1a
    rs = Par(1,5); %[1/min] Splicing rate of XBP1 bionumbers
    rlu = Par(1,6); %[1/min] Translation rate of XBP1u
bionumbers
    rls = Par(1,7); %[1/min] Translation rate of XBP1s
bionumbers
```

```
    rc = Par(1,8); %[1/min] Cytokine production rate bionumbers
    rjnkp = Par(1,9); %[1/min] Phosphorylation rate of JNK
    rjnkm = Par(1,10); %[1/min] Dephosphorylation rate of JNKa
    ra = Par(1,11); %[1/min] Estimated from parameters in
Bionumbers
    ri = Par(1,12); %[1/min] inhibition rate
    dx = Par(1,13); %[1/min] mRNA degradation rate from
Bionumbers
    dl = Par(1,14); %[1/min] protein degradation rate from
bionumbers
    INi = Par(1,15); %[protein/min] Influx of IRE1
    INj = Par(1,16); %[protein/min] Influx of JNK
    ram = Par(1,17);
    rcm = Par(1,18);

    rpp = rpp*signal/20;
    rpm = rpm*signal/20;
    INi = INi*signal/50;
    INj = INj*signal/50;

    x0(1,1) = Par(1,19);
    x0(1,7) = Par(1,20);

    fun = @steady;
    y = fsolve(fun,x0);

    Par(1,i) = 10*Par(1,i);
    rx = Par(1,2)/Par(1,1); %Transcription rate of XBP1
    rpp = Par(1,3); %[1/min]Phosphorylation rate of IRE1
    rpm = Par(1,4); %[1/min] Dephosphorylation rate of IRE1a
    rs = Par(1,5); %[1/min] Splicing rate of XBP1 bionumbers
    rlu = Par(1,6); %[1/min] Translation rate of XBP1u
bionumbers
    rls = Par(1,7); %[1/min] Translation rate of XBP1s
bionumbers
    rc = Par(1,8); %[1/min] Cytokine production rate bionumbers
    rjnkp = Par(1,9); %[1/min] Phosphorylation rate of JNK
    rjnkm = Par(1,10); %[1/min] Dephosphorylation rate of JNKa
    ra = Par(1,11); %[1/min] Estimated from parameters in
Bionumbers
    ri = Par(1,12); %[1/min] inhibition rate
    dx = Par(1,13); %[1/min] mRNA degradation rate from
Bionumbers
    dl = Par(1,14); %[1/min] protein degradation rate from
bionumbers
    INi = Par(1,15); %[protein/min] Influx of IRE1
    INj = Par(1,16); %[protein/min] Influx of JNK
```

```
    ram = Par(1,17);
    rcm = Par(1,18);

    rpp = rpp*signal/20;
    rpm = rpm*signal/20;
    INi = INi*signal/50;
    INj = INj*signal/50;

    x0(1,1) = Par(1,19);
    x0(1,7) = Par(1,20);

    fun = @steady;
    z = fsolve(fun,x0);

    Par(1,i) = Par(1,i)/100;
    rx = Par(1,2)/Par(1,1); %Transcription rate of XBP1
    rpp = Par(1,3); %[1/min]Phosphorylation rate of IRE1
    rpm = Par(1,4); %[1/min] Dephosphorylation rate of IRE1a
    rs = Par(1,5); %[1/min] Splicing rate of XBP1 bionumbers
    rlu = Par(1,6); %[1/min] Translation rate of XBP1u
bionumbers
    rls = Par(1,7); %[1/min] Translation rate of XBP1s
bionumbers
    rc = Par(1,8); %[1/min] Cytokine production rate bionumbers
    rjnkp = Par(1,9); %[1/min] Phosphorylation rate of JNK
    rjnkm = Par(1,10); %[1/min] Dephosphorylation rate of JNKa
    ra = Par(1,11); %[1/min] Estimated from parameters in
Bionumbers
    ri = Par(1,12); %[1/min] inhibition rate
    dx = Par(1,13); %[1/min] mRNA degradation rate from
Bionumbers
    dl = Par(1,14); %[1/min] protein degradation rate from
bionumbers
    INi = Par(1,15); %[protein/min] Influx of IRE1
    INj = Par(1,16); %[protein/min] Influx of JNK
    ram = Par(1,17);
    rcm = Par(1,18);

    rpp = rpp*signal/20;
    rpm = rpm*signal/20;
    INi = INi*signal/50;
    INj = INj*signal/50;

    x0(1,1) = Par(1,19);
    x0(1,7) = Par(1,20);

    fun = @steady;
```

```
    w = fsolve(fun,x0);

    yla = [y.' z.' w.'];
    Par(1,i) = tempPar;

    zla = yla(6,:)./yla(6,1);
    wla(i,:) = zla(1,:).*100;

    figure(i)
    xla = categorical({'Original','Increase','Decrease'});
    bar(xla,yla(6,:));
    ylabel('Concentration (nM)','FontWeight','Bold');
    title(name(1,i));

end
```

PRESENTATION FROM JUNE 9

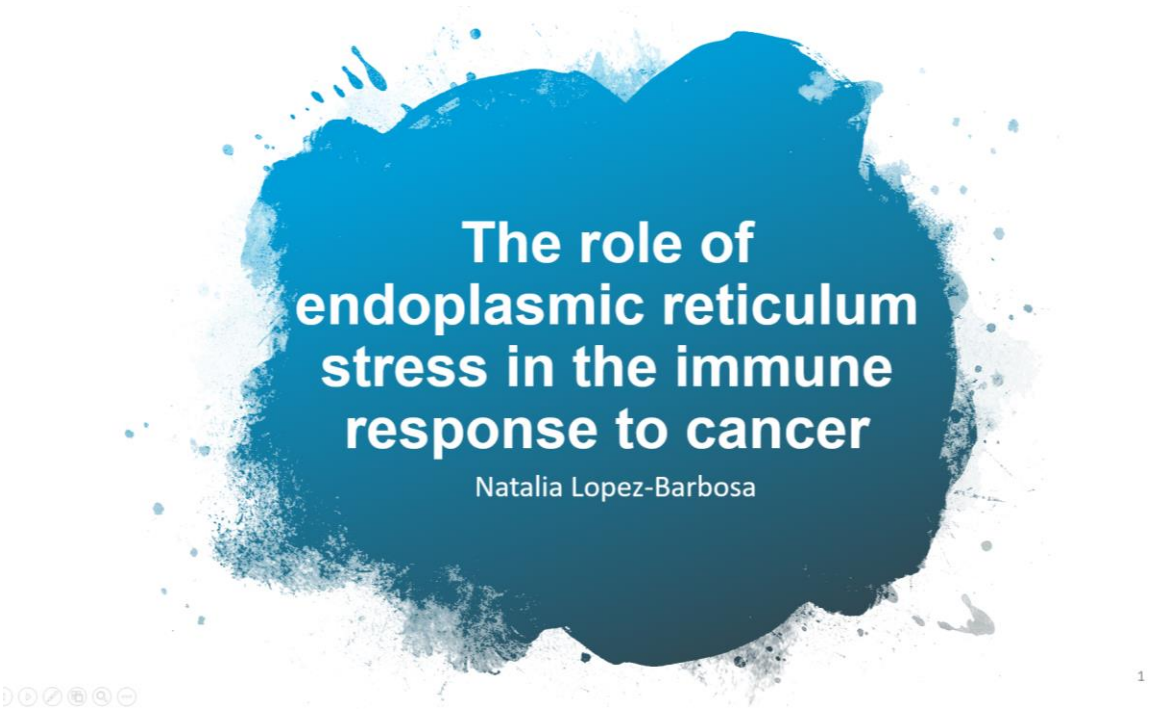

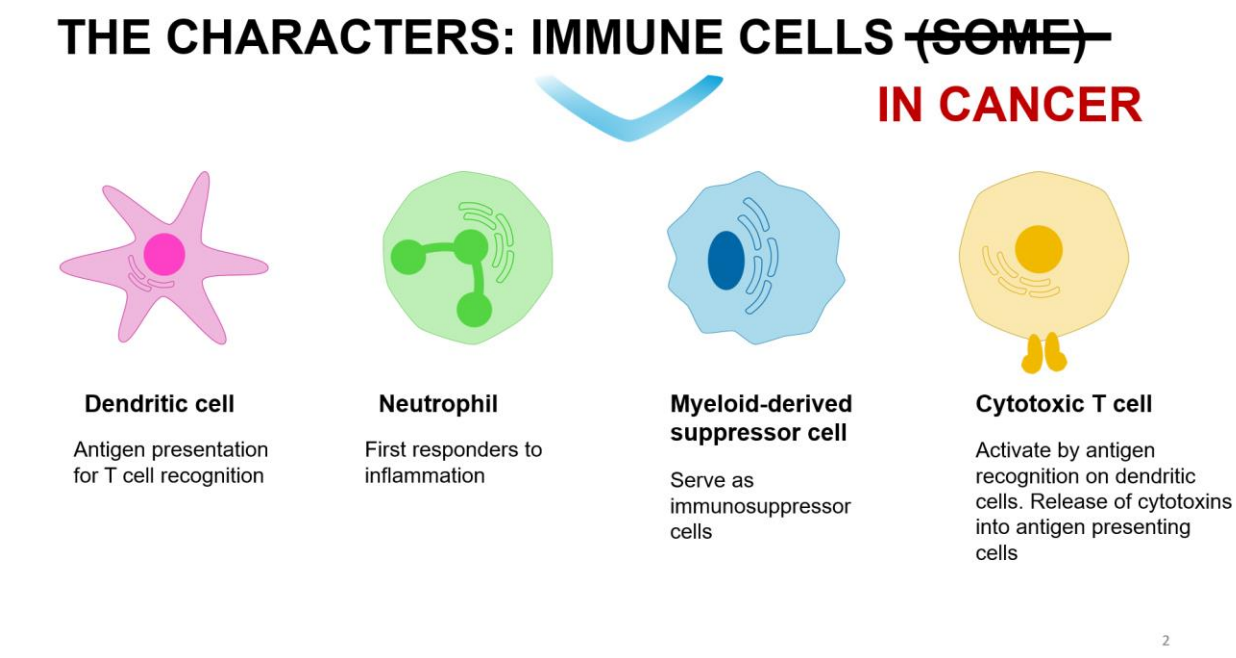

THE BIOLOGY: THE ENDOPLASMIC RETICULUM (ER)

- Organelle found in eukaryotic cells
- Protein synthesis and folding
- Post-translation protein modifications
  - Disulfide bonds
  - N-linked glycosylation

3

THE BIOLOGY: THE TUMOR MICROENVIRONMENT

IMMUNE CELLS IN

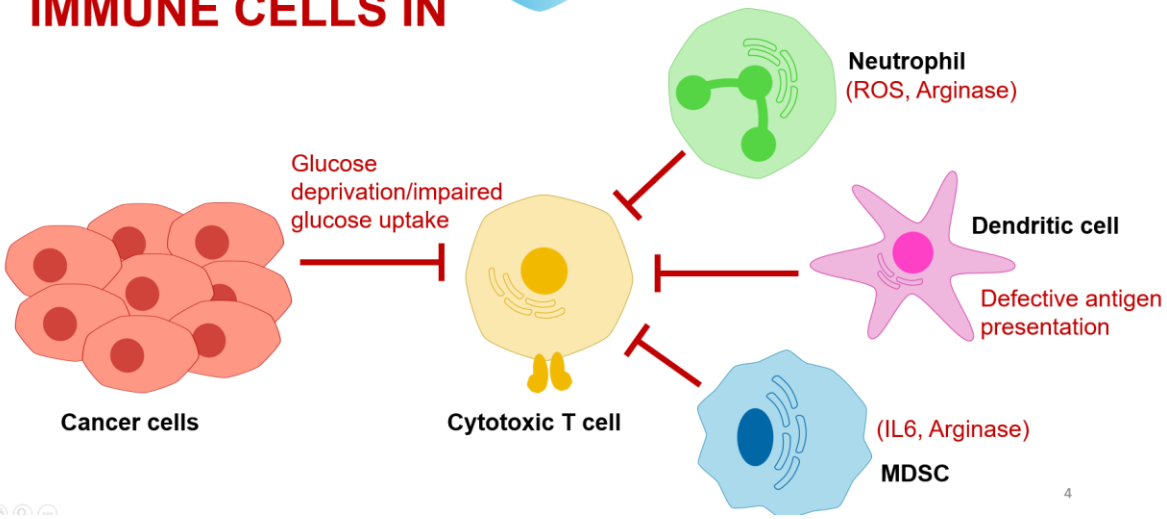

4

THE BIOLOGY: UNFOLDED PROTEIN RESPONSE

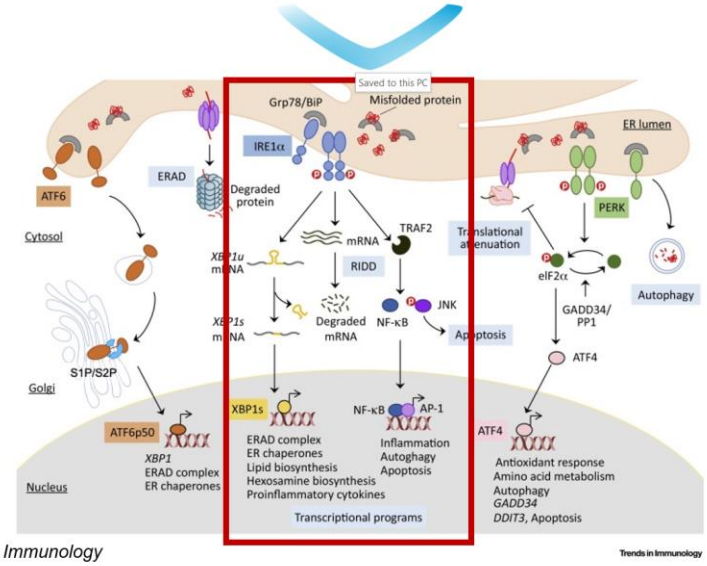

Song et al. (2019) *Trends in Immunology*

5

THE BIOLOGY: UNFOLDED PROTEIN RESPONSE

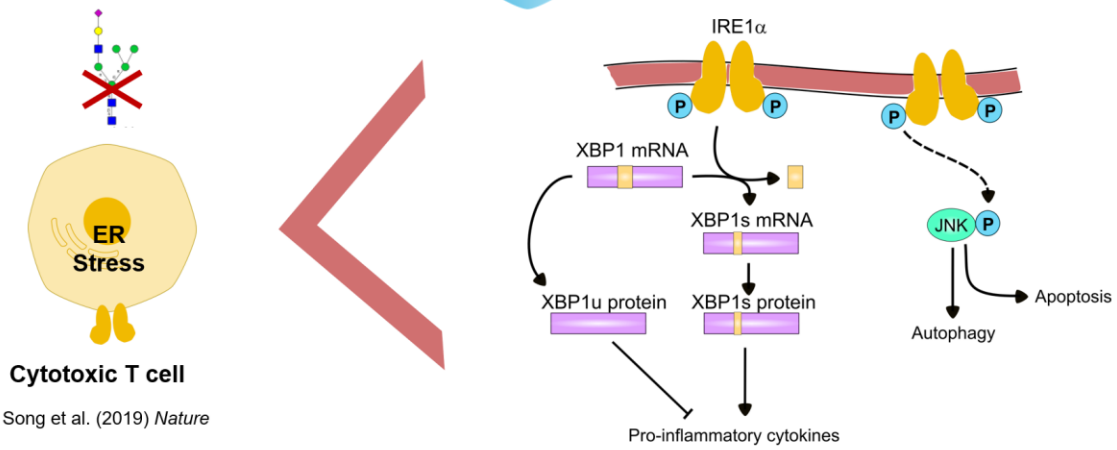

Song et al. (2019) *Nature*

6

THE PAPER

LETTER

https://doi.org/10.1038/s41586-018-0597-x

PATHWAY OF INTEREST!

IRE1α–XBP1 controls T cell function in ovarian cancer by regulating mitochondrial activity

Minkyung Song[1,2,3], Tito A. Sandoval[2,3], Chang-Suk Chae[2,3], Sahil Chopra[1,2,3], Chen Tan[2,3], Melanie R. Rutkowski[4], Mahesh Raundhal[5,6], Ricardo A. Chaurio[7], Kyle K. Payne[7], Csaba Konrad[8], Sarah E. Bettigole[9], Hee Rae Shin[9], Michael J. P. Crowley[1], Juan P. Cerliani[10], Andrew V. Kossenkov[11], Ievgen Motorykin[12], Sheng Zhang[12], Giovanni Manfredi[8], Dmitriy Zamarin[13], Kevin Holcomb[2,3], Paulo C. Rodriguez[7], Gabriel A. Rabinovich[10,14], Jose R. Conejo-Garcia[7], Laurie H. Glimcher[5,6,15]* & Juan R. Cubillos-Ruiz[1,2,3,15]*

THE PAPER: CONCEPTS

ASCITES: Immunomodulatory and tumorigenic fluid that often accumulates in patients with metastatic or recurrent cancer

SPLICING: Removing a piece of mRNA

ACTB: Beta-actin protein. It is often used as a loading control in WB

IFN-γ: Interferon gamma is a cytokine that promotes antigen presentation by MHC molecules

THE PAPER

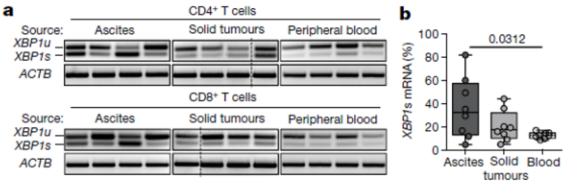

Song et al. (2019) *Nature*

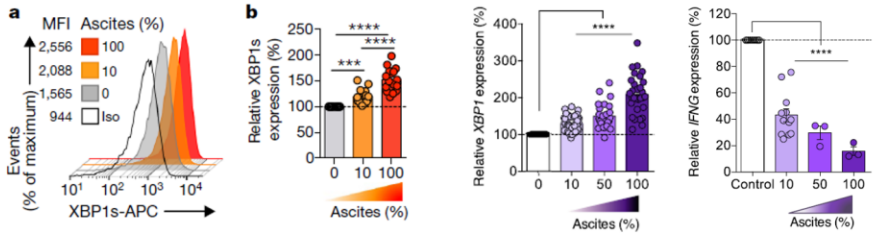

9

MODEL PARAMETERS

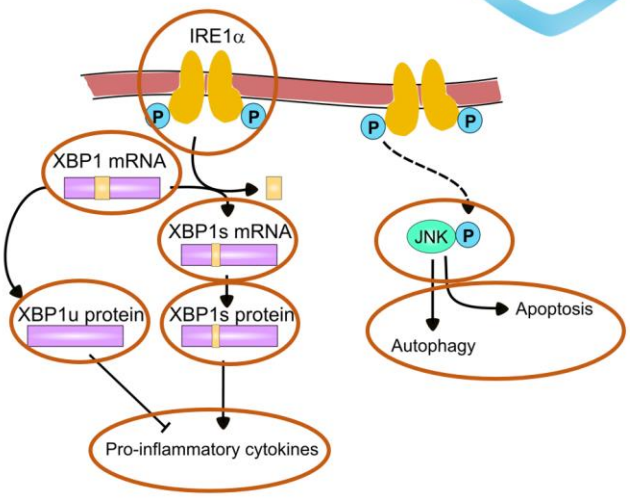

- IRE1, IRE1α
- XBP1 mRNA
- XBP1s mRNA
- XBP1u protein
- XBP1s protein
- JNK, JNKα
- Pro-inflammatory cytokines
- Autophagy and Apoptosis

10

MODEL EQUATIONS

$$\frac{dIRE1}{dt} = r_p^- IRE\alpha - r_p^+ IRE1 - d_L IRE1 + IN_{IRE1}$$

$$\frac{dIRE1\alpha}{dt} = r_p^+ IRE1 - r_p^- IRE1\alpha - d_L IRE1\alpha$$

$$\frac{dmXBP1}{dt} = r_x IRE1\alpha - d_x mXBP1 - r_s mXBP1$$

$$\frac{dmXBP1s}{dt} = r_s mXBP1 - d_x mXBP1s$$

$$\frac{dXBP1u}{dt} = r_{Lu} mXBP1 - d_L XBP1u$$

$$\frac{dXBP1s}{dt} = r_{Ls} mXBP1s - d_L XBP1s$$

$$\frac{dJNK}{dt} = r_{JNK}^- JNK\alpha - r_{JNK}^+ JNK\ IRE1\alpha - d_L JNK + IN_{JNK}$$

$$\frac{dJNK\alpha}{dt} = r_{JNK}^+ JNK\ IRE1\alpha - r_{JNK}^- JNK\alpha - d_L JNK\alpha$$

$$\frac{dCyt}{dt} = r_c^+ XBP1s - r_l XBP1u - r_c^- Cyt$$

$$\frac{dApop}{dt} = r_a^+ JNK\alpha - r_a^- Apop$$

11

STEADY-STATE

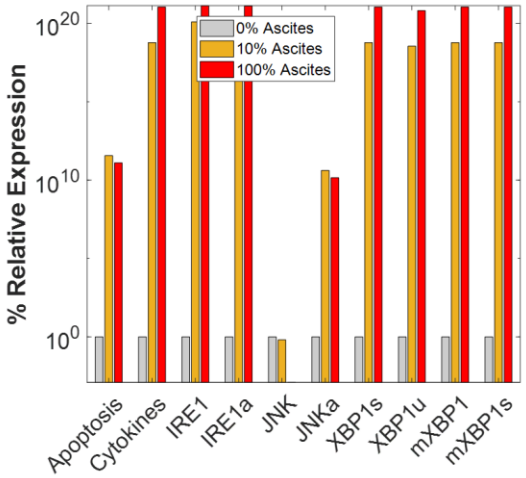

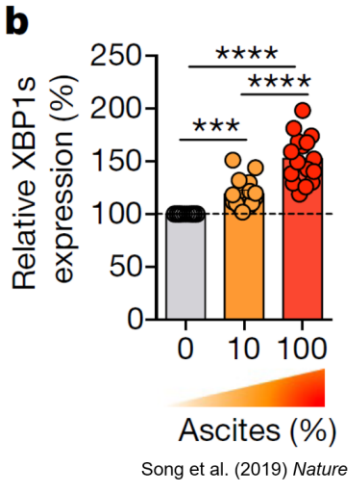

Song et al. (2019) *Nature*

12

FUTURE DIRECTIONS (NEXT WEEK)

Tune parameters

Compare with experimental data

What parameters matter?

13

QUESTIONS?

14